Available online at www.sciencedirect.com
SCIENCE DIRECT®
Journal of the Mechanics and Physics of solids
53 (2005) 597–617
JOURNAL OF THE MECHANICS AND PHYSICS OF SOLIDS
www.elsevier.com/locate/jmps

Insight into the physics of foam densification via numerical simulation

S.G. Bardenhagen[a,*], A.D. Brydon[a], J.E. Guilkey[b]

[a]*Theoretical Division, Los Alamos National Laboratory, Group T-14 MS B214, Los Alamos, NM 87545, USA*

[b]*Department of Mechanical Engineering, University of Utah Salt Lake City, UT 84112, USA*

Received 29 March 2004; received in revised form 3 September 2004; accepted 18 September 2004

Abstract

Foamed materials are increasingly finding application in engineering systems on account of their unique properties. The basic mechanics which gives rise to these properties is well established, they are the result of collapsing the foam microstructure. Despite a basic understanding, the relationship between the details of foam microstructure and foam bulk response is generally unknown. With continued advances in computational power, many researchers have turned to numerical simulation to gain insight into the relationship between foam microstructure and bulk properties. However, numerical simulation of foam microscale deformation is a very challenging computational task and, to date, simulations over the full range of bulk deformations in which these materials operate have not been reported. Here a particle technique is demonstrated to be well-suited for this computational challenge, permitting simulation of the compression of foam microstructures to full densification. Computations on idealized foam microstructures are in agreement with engineering guidelines and various experimental results. Dependencies on degree of microstructure regularity and material properties are demonstrated. A surprising amount of porosity is found in fully-densified foams. The presence of residual porosity can strongly influence dynamic material

*Corresponding author. Tel.: +1 505 665 5323; fax: +1 505 606 0455.
E-mail address: bard@lanl.gov (S.G. Bardenhagen).

0022-5096/$ - see front matter Published by Elsevier Ltd.
doi:10.1016/j.jmps.2004.09.003

response and hence needs to be accounted for in bulk (average) constitutive models of these materials.
Published by Elsevier Ltd.

Keywords: Cellular solids; Foam mechanics; Material point method; Constitutive behavior; Microstructures

1. Introduction

Foamed materials are increasingly finding application in engineering systems on account of their unique structural properties. These properties include physical comfort, effective packaging, and gentle energy absorption. Applications generally involve large material deformations, and may be designed for either static or dynamic response regimes. Examples include seat cushions, impact friendly surfaces (e.g. automobile interiors), energy absorbing structural components, packaging material, and lightweight composite structure components.

Foam mechanical properties are the result of the material's microstructure, a complex three-dimensional network of struts and, possibly, membranes, which undergo large deformations and contact during deformation. The general character of the microstructure of foams allows three regimes of quasi-static, bulk stress–strain compressive response to be easily identified. First is an elastic response at small deformations, during which the network deforms fairly uniformly. Second is a collapse stage where localized bending occurs at weak points in the network. As the structural configuration evolves, new weak points are created and high degrees of bending propagate throughout the microstructure. It is this region which is most characteristic of foams and results in the "stress plateau" where large displacements occur at essentially constant force. Finally, there is a densification phase when the network is collapsed onto itself and contact between network elements results in a dramatic stiffening of the material.

These regimes of deformation have been studied extensively and significant understanding has been obtained using idealized models. However, as with other complex "microstructured" materials, developing an understanding of the correspondence between characteristics of the microstructure and the bulk response is a grand challenge. Decades of experimental work on foams has served to demonstrate the complexity of foam deformation and offer many insights into the relationship between microstructure geometry and material properties on foam bulk response Gibson and Ashby (1997). More recent work has provided detailed microstructural deformation information at given bulk deformations Zhu et al. (1997), Kinney et al. (2001), Smith et al. (2001). However, separating effects due to microstructural geometry from those due to microstructural material properties remains exceedingly difficult. The foaming process allows for only limited control of the resulting microstructure geometry, and, for many foams, foaming is part of curing process which determines the microstructure material properties, i.e. there is no corresponding "bulk material".

This situation would seem to be fertile ground for numerical simulation. Many researchers have turned to numerical simulation to gain insight into the relationship between foam microstructure and bulk properties Zhu et al. (1997), Zhu and Windle (2002), Shulmeister et al. (1998), Vajjhala et al. (2000), Chen et al. (1999), Meguid et al. (2002). However, simulating foam mechanical response at the microstructural level is a well established computational challenge for at least three major reasons. First, the complexity and variety of realistic foam initial microstructures is effectively a subject in rheology in itself Kraynik (2003). Sophisticated analysis and computational tools are required to generate representative geometries. In order to simulate material response, these microstructures must be discretized. Even idealized foam microstructures are difficult to discretize with a body-fit mesh. More realistic geometries, obtained from X-ray tomography for example Smith et al. (2001), are more difficult.

Second, foams are required to operate in the stress plateau and densification regimes to make use of their unique mechanical properties. Hence, the material deformations of interest are large, both on average (i.e. bulk) and at the microscale. Even at moderate bulk deformations, e.g. within the stress plateau, localized bending at the microscale results in large deformations and rotations of the individual structural components (struts, membranes). Hence finite deformation continuum mechanics formulations must be implemented, including appropriate kinematics and constitutive models. Large strains result in numerical inaccuracies as Lagrangian meshes become too distorted or Eulerian meshes require extensive material advection.

Finally, the transition from stress plateau to densification regimes is driven by self contact of the collapsing foam microstructure. Contact algorithms themselves are an area of ongoing research Zhong and Mackerie (1994). Simulation results are often found to be strongly dependent on the specific values of the algorithm's parameters, which are generally only loosely tied to material properties. Common algorithms, such as master and slave, require the identification a priori of candidate contact surfaces, which is only possible early in the deformation for foam microstructures, if at all.

The combination of discretizing complex microstructures and simulating large deformations and contact is extremely challenging numerically for the finite element method (FEM), easily the most widely used numerical solution procedure in solid mechanics. Consequently, foam micromechanics simulations with FEM have been forced to focus on modest deformation foam behavior Zhu et al. (1997), Zhu and Windle (2002), Shulmeister et al. (1998), Vajjhala et al. (2000), Chen et al. (1999), Meguid et al. (2002).

Remarkably, this same combination of numerical simulation challenges plays directly into the strengths of certain particle methods. Recent developments in particle-in-cell (PIC) methods indicate that these numerical techniques are suitable for precisely this class of problem Bardenhagen et al. (2001), Bardenhagen and Kober (2004). Calculations are presented here in which, for the first time, simplified foam microstructures are compressed well into the densification regime. Macroscopic stress–strain curves agree qualitatively with experimental results and

engineering estimates of key deformation material response parameters. Material properties and microstructure geometries are varied independently and the results are reported. Analysis of the deformed configurations indicates a surprising degree of porosity remains in fully densified foam microstructures.

Of interest in this investigation is a better understanding of the physics of foam deformation, particularly in the densification regime. Their response over a range of deformation rates, from quasi-static to strong shock, is not well understood. Improved bulk (''average'') constitutive models for foams are needed to analyze systems in which they are structural components. Micromechanical simulations of foam response provide a tool to improve the bulk models, guiding the incorporation of important microstructural features. The simulations presented here suggest porosity is an important microstructural feature which must be accounted for (independently of bulk strain) by bulk constitutive models operating in the densification regime.

2. Numerical technique

PIC methods were originally developed in computational fluid mechanics to model highly distorted fluid flow Harlow (1963). Subsequent developments advanced the understanding of the algorithm and reduced numerical diffusion Brackbill et al. (1988), Burgess et al. (1992). More recently the natural role of the particles, or ''material points'', in handling constitutive response state variables was recognized, and a modified algorithm, the material point method (MPM), was applied to computational solid mechanics problems Sulsky et al. (1994, 1995). Recent developments in MPM have addressed accurate and robust handling of material contact Bardenhagen et al. (2000, 2001). Most recently, a general mathematical framework was identified, the generalized interpolation material point method (GIMP method) Bardenhagen and Kober (2004), which allows MPM to be derived as a special case. The GIMP method framework addresses accuracy in handling large material deformations, and identifies similarities with the ''meshless methods'' particle methods Belytschko et al. (1996), Babuška and Mellenk(1997), Demkowicz and Oden (1986), Atluri and Zhu (2000).

In GIMP material bodies are discretized into material points which carry all material properties and state. This includes constitutive parameters, such as internal variables, and state variables, such as stress, strain, velocity and temperature. In short, everything required to specify the current material state and advance the solution is carried on the particles. They also serve to implicitly track material interfaces. Discretization of complex material shapes is straightforward. A regular grid of candidate material point positions is generated. At positions found to lie inside a given body material points are generated. The resulting discretization is similar to using pixels to represent an image.

The algorithm also uses an overlying grid to which relevant particle information is interpolated. Updated Lagrangian conservation of momentum equations are solved on this computational scratch pad (Conservation of mass is satisfied implicitly by

holding particle masses constant). Updates are interpolated to the particles, after which the grid is discarded. A new grid is generated each computational time step, providing the flexibility to change (refine or coarsen) the mesh as advantageous, and eliminating mesh tangling problems. For the calculations presented here the grid is reset to it's original configuration each timestep for simplicity and hence appears stationary in space, or "Eulerian".

The brief description above is only intended to provide a basic understanding of the nature of the algorithm. It is an ALE technique, often described as Lagrangian particles moving through an Eulerian mesh. The method may be derived from the principle of virtual work via a Petrov–Galerkin discretization scheme, a more general scheme than used in the FEM. The method uses a grid to interact particles, as opposed to pairwise interactions as used in Smooth Particle Hydrodynamics. The interested reader is referred to the references in this section for algorithmic details.

3. Numerical simulations

Numerical simulation of realistic foam microstructures over the full range of bulk compression in which these materials operate in applications is an established computational challenge. The primary goal of this manuscript is to establish a convincing capability perform these simulations. Relatively simple unit cell approximations to foam microstructures are considered in order to lay the groundwork for future simulations of the computational scale and geometric complexity required to approximate real foams. A primary focus is on validation. The wealth of experimental data on foams already available allows qualitative comparisons with simulation results to be made. Established engineering guidelines are also used to evaluate the results. Recent "microscale" measurements including the response of single foam pores Zhu et al. (1997), and measured porosity during compression Smith et al. (2001), provide further validation information.

It should be noted that elastic material models and no-slip contact are used in these simulations. For polymeric foams these are probably reasonable approximations. The philosophy adhered to is to include sufficient model complexity to credibly model foam compression into the densification regime. Hence these simulations include network microstructures, finite deformation constitutive response, and contact between arbitrary network components. It is demonstrated that attending to these essential features of foam mechanics results in simulation data remarkably similar to real materials. It also provides a baseline for future numerical simulations. Effects due to including more realistic models, such as viscoelasticity for polymeric foams, plasticity for metallic foams, and frictional sliding contact, will be studied later.

A secondary goal is to demonstrate the power of the computational machinery by exploring the influence of microstructure geometry and material properties (independently) on bulk response. The results presented here give only preliminary indications of the effect of varying these parameters in real foams. The study of real foams requires the generation of realistic geometries and the simulation of much

larger microstructures. This is a complex problem which has received attention for open cell foams by considering soap froths Kraynik (2003). Another promising means of obtaining realistic initial geometries is via X-ray tomography Kinney et al. (2001), Smith et al. (2001) and it is noted that, for a particle method, an array of pixel intensities representing an image can be easily discretized.

GIMP methods have been applied primarily in dynamics where inertial forces, material strain rate effects, and stress wave propagation are of primary interest. Hence explicit solution schemes for GIMP algorithms are the most developed. Dynamic simulation scenarios are ultimately of interest in this investigation, which is targeted at improving both the understanding of, and the engineering (''bulk'') modeling capability for, the dynamic response of foams used in defense applications. However, most experimental data on foams, and particularly that for open cell foams most like the idealized unit cells considered here, are for quasi-static response. To simulate quasi-static deformations an implicit numerical solution strategy is generally preferred. Currently these algorithms are expensive, and remain an area of algorithm research for GIMP methods Cummins and Brackbill (2002), Guilkey and Weiss (2003). While less elegant, it is also possible to obtain quasi-static results with an explicit code provided the loading is applied slowly enough. This is the approach pursued here toward validating the modeling capability.

In Section 3.1 compression of microstructure constituent material is examined to establish appropriate simulation parameters for quasi-static results and provide a reference constitutive response to compare with the bulk response of the foams. Section 3.2 gives detailed results for two foam microstructures, permitting effects due to microstructural geometry and material properties to be studied independently. Analysis of the deformed configurations reveals a surprising amount of residual porosity in fully-densified foams.

3.1. Constituent material response

The first simulation objective was to demonstrate that the explicit computation algorithm can give good results for large quasi-static deformations provided the loading is applied slowly enough. A compressible Neo-Hookean (nonlinear) elastic formulation was selected for the microstructure material constitutive response Simo and Hughes (1998). This is a large deformation constitutive model appropriate for natural rubbers and for polymers in which viscous response is not expected to be large. The material parameters used are a bulk modulus of 10.2 GPa, a shear modulus of 7.2 GPa, and a density of 1900 kg/m^3.

Fig. 1 depicts stress–strain curves for uniaxial strain, constant strain-rate deformation of a solid cube of this material. Both an analytic solution (dashed line) and a numerical solution (solid line) are presented. The analytical solution is the static response of the material as calculated using the Neo-Hookean constitutive model under uniaxial strain deformation. Note that the material model stiffens dramatically at large compressions, a realistic aspect of large compression material response. The numerical result is obtained as for a typical experiment on foams. A piston is used to compress the material at constant speed and the load required is

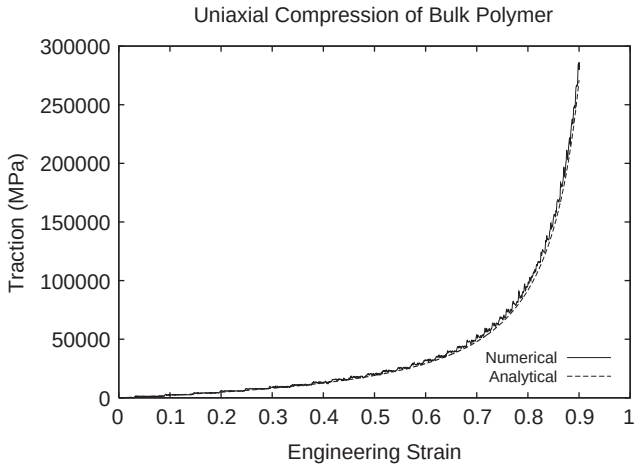

Fig. 1. Comparison of analytical and numerical solutions of the uniaxial compression of compressible Neo-Hookean material.

measured. The traction is calculated as the load (defined as positive in compression) divided by the area over which the load is measured, and the engineering strain is the change in length of the specimen divided by its initial length (also defined as positive in compression).

Because the material response is not rate dependent, in the absence of inertial effects and numerical discretization errors, the numerical solution should be identical to the analytical one. In order to obtain quasi-static results, the piston velocity is prescribed to be a small fraction of the material wave speed, and the total simulation time is long relative to the time required for a stress wave to propagate across the block. For this simulation the piston speed is 3% the initial longitudinal wave speed, and the total simulation time required for 90% compression is 30 times the wave propagation time. In addition, artificial viscosity is added to the calculation to damp out numerical ringing at wave fronts. The numerical solution is for a 1 mm^3 block of material and uses 0.01 mm cell size discretization.

For these simulation parameters quite good agreement is found between numerical and analytical results. At the highest strain the numerical solution error is approximately 5%, and this is for the case when *all the material points are compressed into one-tenth the initial volume*. To provide some perspective, if a uniform body-fit (cubic) grid were used, the final deformation would result in cell aspect ratios of 10. For the contiguous particle GIMP method used here there are small errors associated with particles crossing computational cell boundaries, resulting in the spikes in the numerical result evident at large strains. The interested reader is referred to Bardenhagen and Kober (2004) for details. Here it is simply noted that the numerical solution is accurate for larger strains than are expected in the compression of the foam microstructures (which are approximately 90% void).

3.2. Foam unit cell calculations

Foams are characterized in detail by the geometry of the network of struts and membranes which make up the microstructure, and the pointwise material properties of the network. More coarsely, foams are characterized by the network material properties, assumed uniform, and the foam's relative density, $\phi = \rho_{\text{foam}}/\rho_{\text{solid}}$, where ρ_{solid} is the density of the network material. These properties may be used to derive bulk foam material properties and how they vary Gibson and Ashby (1997). However, they are estimates of bulk foam properties, and are only approximate. In particular they are independent of the geometry of the foam microstructure, with the exception of distinguishing between open and closed-cell foams. Furthermore, practical difficulties arise when there is no corresponding un-foamed material, as is clearly the case when the foaming process is also part of the curing process. Generally foam properties can be expected to vary within the network due to processing irregularities or as network dimensions approach material scales (e.g. grain size in metals or filler size in polymers). The understanding of these complex materials could be improved via realistic numerical simulations where the effects of microstructure geometry and material properties may be varied independently.

Higher relative density foams, with partially or fully closed cells, have especially complicated microstructures, including thin membranes partially and completely isolating individual cells. Furthermore, trapped gas and gas flow can play a role in the material response, especially at high deformation rates. For the baseline calculations presented here relatively simple microstructures were used, more characteristic of open celled, low relative density foams, $\phi \approx 10\%$, such as might be used in seat cushions.

Two idealized foam microstructures are considered here, see Fig. 2. The compressing piston is black and provides a constant velocity boundary condition. The bottom boundary is a symmetry plane and the remaining (in-plane) boundary conditions are periodic. The simulations correspond to the compression of an infinite, periodic, two unit cell thick layer of foam. On the right in Fig. 2 is a foam microstructure created by perturbing a regular structure. The perturbations are in the positions of the spherical nodes, which are initially at the vertices of a regular lattice. The nodes are randomly shifted a distance of 3–8% of the unit cell size. This

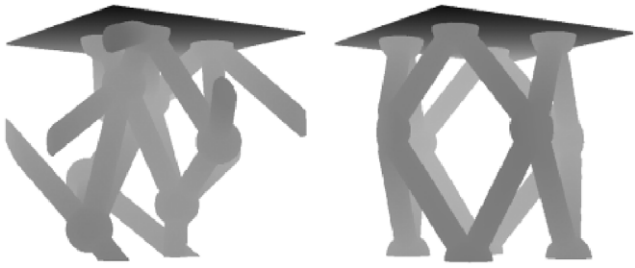

Fig. 2. Unit cell initial configurations of the two foams constructed for study. The random unit cell is depicted on the left and the lattice unit cell on the right.

microstructure is referred to as the "lattice" and has $\phi = 7.9\%$. The second microstructure in Fig. 2 is a pseudo-random structure generated by hand. It was constrained to be periodic, and to have a similar relative density as the lattice. This microstructure is referred to as "random" and has $\phi = 9.6\%$.

The foam microstructures were compressed well into the densification regime using the same compression rate and discretization specified in Section 3.1. Because both unit cells are approximately 90% void, compression to 90% engineering strain will serve first to collapse the microstructure and remove void space, and second to compact the collapsed structure. The maximum compression simulated is essentially that required to remove all void space from the microstructure, or "fully densify" them (assuming incompressibility).

The bulk responses of the foam unit cells are depicted in Fig. 3, where the compressive traction and engineering strain are reported over the entire range of compression simulated. The structures stiffen so dramatically that material response at small and moderate compressions is not discernible. This dramatic stiffening is the signature of compression in the densification regime where contact mechanics plays an important role. The random foam reaches the densification regime at slightly smaller strains primarily on account of its slightly higher relative density. While the general character of the traction/strain curves is similar to that of the network material, i.e. Fig. 1, the maximum tractions registered for the foams are approximately two orders of magnitude lower.

The first 70% strain, for the random unit cell, is shown in Fig. 4 with a dashed line. On this scale, the data is somewhat "noisy". The traction measurement is made on the bottom computational boundary. This measurement registers the arrival of stress waves which have propagated through the structure, as well as collisional events which occur as additional struts make contact with the bottom boundary. The "noise" in the stress–strain curve due to additional struts contacting the boundary

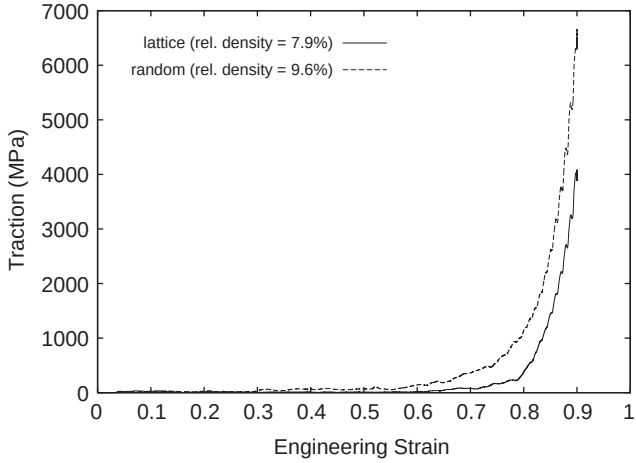

Fig. 3. Response of the two foam microstructures to quasi-static uniaxial compression.

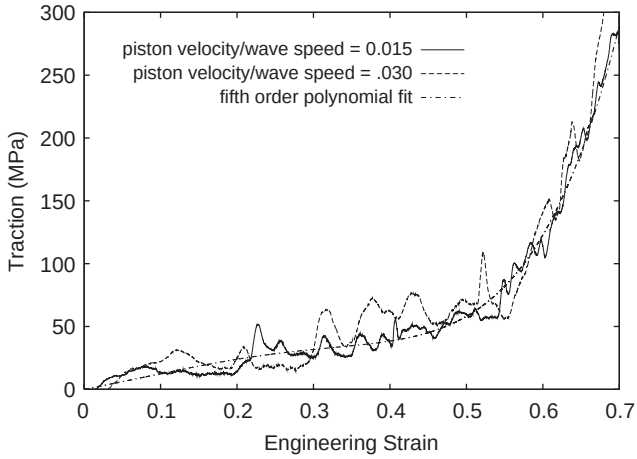

Fig. 4. Response of the random foam microstructure compression at two rates and a polynomial fit to the data.

accurately reflects the physical process of microstructure collapse and densification. The magnitude of these fluctuations is an artifact of the small unit cell size. Simulations of larger microstructures will have a higher frequency of strut contact events of similar magnitudes, but divided by a larger measurement area. Hence the bulk response curve is expected to be smoother for larger microstructures. Nevertheless, the stress plateau and densification regimes are easily distinguished in the data, indicating that the random unit cell is behaving qualitatively like a foam.

The foam unit cell calculations involve structural collapse, potentially an inertial process, in addition to stress wave equilibration. An additional simulation, at half the compaction velocity, was also performed to assure that inertial effects are minimized. The results of the slower compression simulation are displayed with a solid line in Fig. 4. The responses for both rates are similar. A smooth fit to the data using a fifth order polynomial (depicted with a dash–dot line) can be expected to be a reasonable representation of the bulk static stress–strain curve for the random microstructure. The magnitude of the excursions from this fit are generally smaller for the lower strain rate simulation as would be expected as strut/boundary "collisions" become more mild. It is concluded that the faster piston speed gives representative quasi-static results, and this speed is used for all remaining simulations.

The quasi-static bulk compressive response of the lattice unit cell is depicted in Fig. 5 over the first 70% strain. The range of tractions displayed is identical to the previous figure for the random unit cell, emphasizing the differences in bulk response on account of the differences in microstructures. The lattice unit cell has a much flatter stress plateau. A polynomial fit through the data is also displayed.

To simplify the comparison only the traction-strain polynomial fits are depicted in Fig. 6. The three regimes of deformation characteristic of these materials are easily

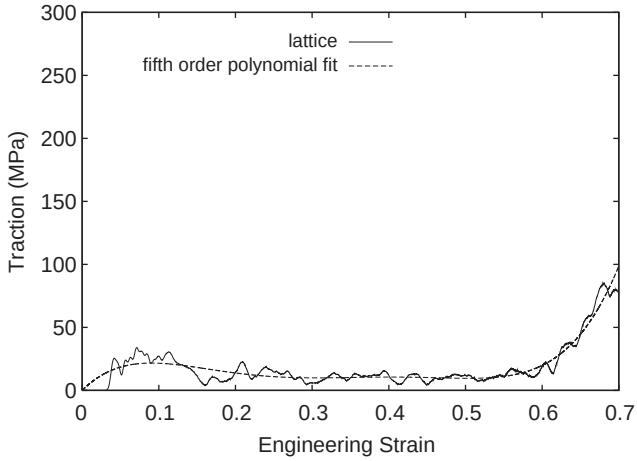

Fig. 5. Response of the lattice foam microstructure to quasi-static uniaxial compression and a polynomial fit to the data.

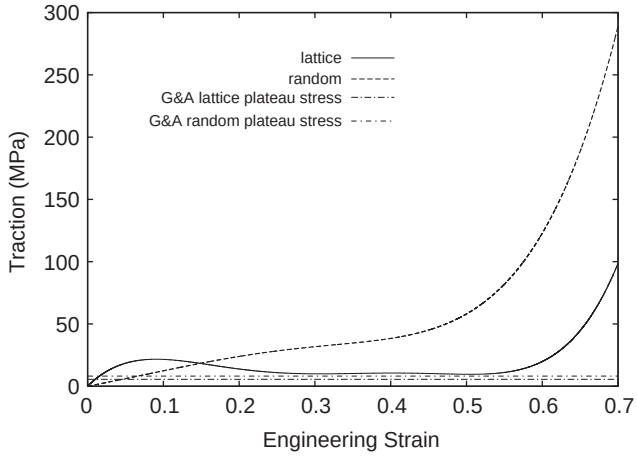

Fig. 6. Approximate quasi-static response of both microstructures and yield stress estimates from the formulas of Gibson and Ashby.

identified, indicating the numerical simulations exhibit qualitatively correct bulk foam behavior. Horizontal lines are drawn in Fig. 6 at the "yield" stress predicted by the formulas of Gibson and Ashby (1997). This stress is computed using only network material properties and foam relative density, ϕ. Characterization of foam microstructure regularity does not enter the equation. The formula has been found to be a remarkably good approximation, for most foams, of the stress which marks the beginning of the transition to the stress plateau. Hence it is a softening, or

"yield" stress. These numerical simulations results are as consistent with this guideline as many experimental data.

An important difference between the bulk behavior of the two microstructures may be identified in Fig. 6. The nearly perfect lattice microstructure has a much flatter plateau region than the random one. The drop in traction with increasing strain suggests collapse to a more compressed unit cell configuration which carries less load. This result is consistent with the buckling of regular structures which, if unstable, dynamically "snap-through" to a post-bifurcation solution. Precisely this mechanism has been used in the development of bulk foam constitutive models which predict heterogeneous strain states under uniform compressive stress Wang and Cuitiño (2000), Gioia et al. (2001). For the random microstructure the response is monotonic.

The compaction of the foam microstructures quasi-statically is depicted at various stages of deformation in Fig. 7. Material points are plotted, colored by a norm of the stress tensor, the "equivalent stress" ($\sigma_{\mathrm{eq}} = \sqrt{1.5\sum_{ij}\sigma'_{ij}\sigma'_{ij}}$), where σ' is the stress deviator. This measure emphasizes regions of high shear. Material point values above a threshold value are all plotted in red to emphasize high stress regions. The same color bar range is used for both microstructures and all deformations. Note that for both microstructures the material fraction at a given equivalent stress appears similar at corresponding compressions, suggesting that similar microscale deformation mechanisms are occurring.

In the top frames in Fig. 7 the engineering strain is 10%. The stress distributions in the microstructures clearly indicate the foam response is dominated by bending and strut junction stiffness, even at this relatively low strain. That strut bending continues to dominate the response at larger deformations (30% and 50% engineering strain) is apparent both from stress distributions and deformed geometries. The amount of material most highly stressed slowly increases with increasing strain as the struts become increasingly contorted. At 70% engineering strain strut contact is extensive and low stress regions are beginning to disappear, suggesting the microstructures are in the densification phase of deformation. That this is the case can be confirmed from Fig. 3. The final configuration, at 90% engineering strain, is displayed as viewed from below, and no low stress regions remain.

The obvious difference between the deformation of the two microstructures is the progressive loss of geometric regularity for the lattice. The contorted state at 30% strain maintains a degree of order suggestive of an anti-symmetric buckling mode. By 50% strain this order appears to be essentially lost. The process of losing regularity has the potential to result in a dramatic change in response, as it is akin to buckling. The perfect version of this microstructure must admit solutions with planes of symmetry in the lattice directions. Loss of symmetry occurs when the structure buckles, after which the character of the deformation is determined by the post-buckling solution, which may even be unstable, resulting in snap-through behavior. The (imperfect) lattice microstructure simulated here does not buckle per the mathematical definition, but it does exhibit a similar rapid change in solution character. This change is evident between 10% and 30% strain in Fig. 7. Based on

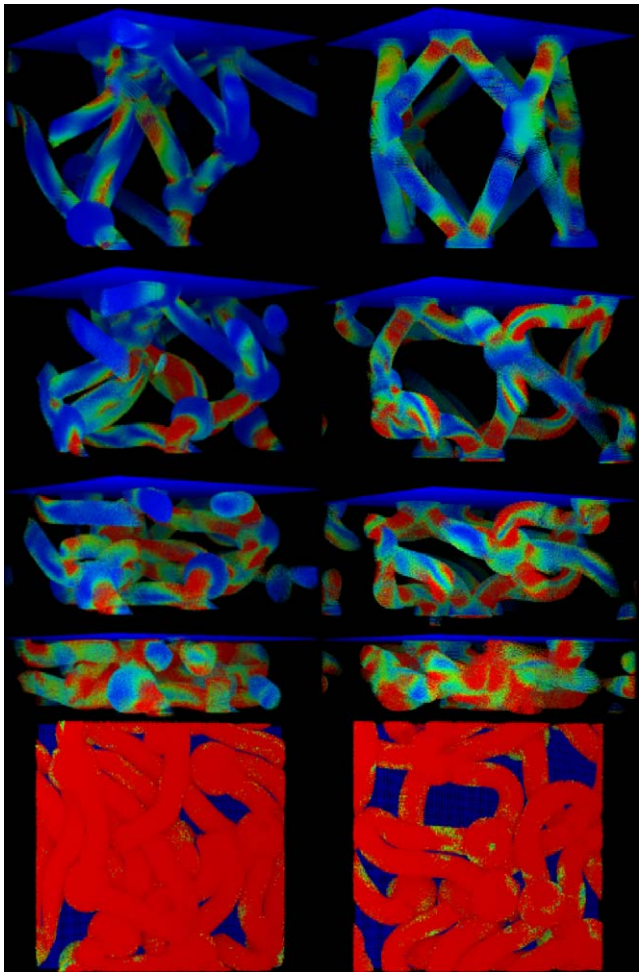

Fig. 7. Deformation of the random (left) and lattice unit cells. The frames are at 10%, 30%, 50%, 70% and 90% engineering strain from top to bottom (with the bottom frame viewpoint from below). Material points are colored by equivalent stress.

the bulk behavior depicted in Fig. 6, which exhibits a maximum load in this strain range, the change is associated with snap-through. In contrast, the random structure has no symmetries to break and it's bulk behavior is monotonic.

Experiments have been performed on single foam pores Zhu et al. (1997). Compressive tractions as a function of engineering strain were measured, as in these simulations. For the two unit cells for which experimental data was presented, one had a very flat stress plateau very much like the lattice simulation as depicted in Fig. 6. Images of the undeformed and deformed pores were also presented. There is a degree of symmetry and order to the undeformed pores which is also suggestive of

the lattice unit cell. It is very interesting to note that for the case with the flat stress plateau a disruption of this regularity is clearly evident in the deformed configuration. The other bulk pore traction–strain response was monotonic. For that case the deformed configuration maintained its initial symmetry, probably largely on account of boundary conditions. The pores were glued to the compressing plates. The same monotonicity has also been found in numerical simulations Shulmeister et al. (1998) for larger unit cells which maintained their symmetry under compression. Here it is argued that these results are not representative of real foam pore collapse where imperfections lead to high degrees of bending in general, and possibly local snap-through behavior for sufficiently ordered structures.

Although it is tempting to suggest the results in Fig. 6 are representative of bulk foams with similar microstructures, it is unlikely to be the case. Much bigger unit cells need to be considered Zhu et al. (1997), Shulmeister et al. (1998), Zhu and Windle (2002). Accurate determination of bulk foam response requires finding the necessary size of a representative volume element (RVE) of material. This is not to suggest sensitivity to variations in microstructure disappear for sufficiently large RVEs. Bulk property sensitivity to variations in microstructure, even for the same relative density, are also well established Zhu and Windle (2002), Kraynik (2003), Vajjhala et al. (2000), Chen et al. (1999).

Having established that the responses of the two unit cells are reasonable, it is informative to extract information regarding the deformation at the microscale. Because material deformation is tracked at each material point, it is possible to extract the porosity throughout the simulation. The porosity, p, is defined as

$$p = \frac{V_{\text{bulk}} - V_{\text{microstructure}}}{V_{\text{bulk}}}, \tag{1}$$

where V_{bulk} is the volume under the piston, or the "bulk" foam volume and $V_{\text{microstructure}}$ is the volume occupied by the foam microstructural network. The porosity of the two unit cells as a function of engineering strain is presented in Fig. 8. The porosity of an incompressible foam, where $V_{\text{microstructure}} = \text{Const.}$, may be expressed in terms of the relative density and engineering strain, ε_{eng},

$$p_{\text{inc}} = 1 - \frac{\phi}{1 - \varepsilon_{\text{eng}}}. \tag{2}$$

The incompressible foam microstructure porosity is also presented in Fig.8.

Both microstructures are approximately incompressible initially. For the random case, at larger deformations, the actual porosity is consistently greater than the incompressible estimate, which is consistent with expectations for compressive bulk deformation and material compressibility. The actual porosity diverges significantly from the incompressible estimate as the microstructure becomes pinned near full densification and porosity is "locked in". For the lattice case, in the stress plateau and early densification regimes the porosity is less than the incompressible estimate. This is likely due to competition between regions of compression and tension during snap-through of this microstructure. In the densification regime the actual porosity eventually becomes greater than for the incompressible case, again due to material

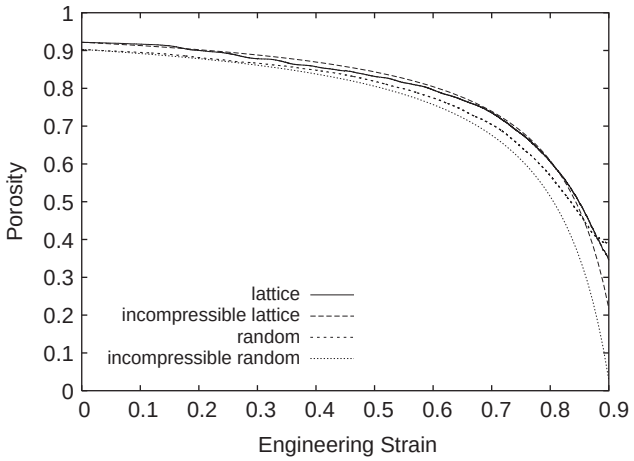

Fig. 8. Porosities of the two foam microstructures during compression from the simulations and calculated assuming incompressibility.

compressibility and locking in pore space. The residual porosity at the end of the calculations may be clearly seen in the bottom frames of Fig. 7.

The presence of significant residual porosity at full densification is consistent with recent experimental work on foam using X-ray tomography Smith et al. (2001). There an open cell foam of initial porosity 48% was found to contain 13% porosity under uniaxial compression to $\varepsilon_{\text{eng}} = 0.5$, which is near full densification. These same experiments indicate that 6% porosity remains for $\varepsilon_{\text{eng}} = 0.6$, which is well *past* full densification. For the numerical simulations, which are initially approximately 90% porous, about 35% porosity is retained near full densification. Clearly details of contact geometry and material properties will strongly influence residual porosity. Most importantly, the simulations capture this important physical feature.

A tempting engineering assumption is that foams will have had all porosity removed at full densification. Hence, while the stress state is clearly non-uniform, the material may be approximated as a continuous solid. In fact, porosity is not easily removed from these materials under quasi-static deformation. The fact that substantial porosity is retained at full densification has significant implications for the dynamic response of these materials. Stress wave propagation is strongly affected by the degree of material heterogeneity Legius et al. (1997). Void space represents one extreme of material property contrast. Wave reflection at voids results in an irregular wave front and, possibly, dispersion. Consequently, the assumption that foams are essentially incompressible would be significantly in error near full densification, and would result in completely overlooking important physical processes.

Having identified microstructural geometry effects, material property effects were investigated. Fig. 9 indicates the response of the two unit cells when the material constants are doubled. At any given strain the stiffer foams support approximately

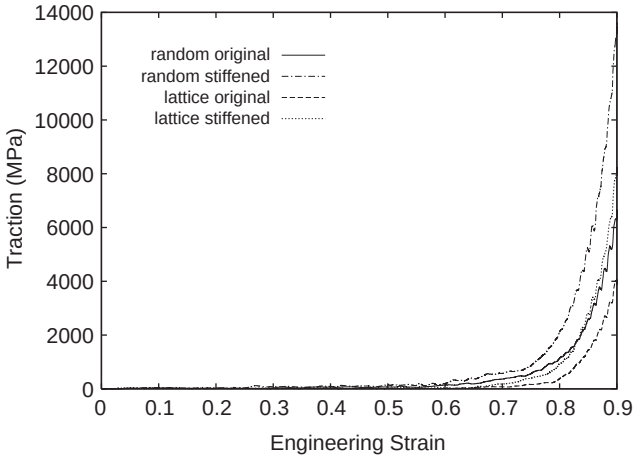

Fig. 9. The effect of doubling the material constants on the response of the two foam microstructures.

twice the load. This suggests the collapse and densification process is the same for a given microstructure, with the pointwise stress everywhere simply a factor of two larger for the foam with stiffer material. While this result was expected at small compressions, where the bulk response is due strictly to the constitutive response of the network material, it seemed plausible that finite deformation contact mechanics might disrupt such a simple relationship. Given only two examples it is not conclusive, but it appears the bulk response scales with the network constitutive response as could be predicted based on Hertzian contact mechanics.

Another interesting feature in Fig. 9 is that the curve for the stiffer lattice unit cell crosses the curve for the softer random unit cell. This indicates a subtle dependence on unit cell geometry, distinct from the dependence on initial relative density, in the densification regime. The details of the collapse process clearly depend on the initial network configuration. Apparently the collapse process for the lattice unit cell results in a less efficient packing of material during densification than the random unit cell. An qualitative indication of packing efficiency may be seen in the bottom frames of Fig. 7, where much larger pore spaces are found in the lattice unit cell, suggesting more strut overlap has occurred in the densification of that microstructure.

Fig. 10 focuses on the first 70% strain for the random unit cell. Simulation results as well as polynomial fits are shown. Here the stress plateau and beginning of the densification regimes are easily identified. The polynomial fits suggest the stiffer foam supports twice the load at moderate strains as well. Fig. 11 focuses on the first 70% strain for the lattice unit cell. Simulation results as well as polynomial fits are shown. Again the stress plateau and beginning of the densification regimes are easily identified. Here it is less clear that the stiffer foam supports approximately twice the load early in the stress plateau region. This region is associated with the snap-through process which, if unstable, will be dominated by inertial effects. The

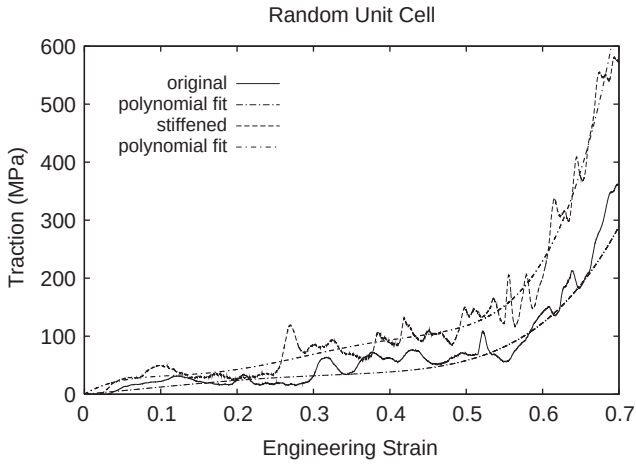

Fig. 10. The effect of doubling the material constants on the response of the random microstructure.

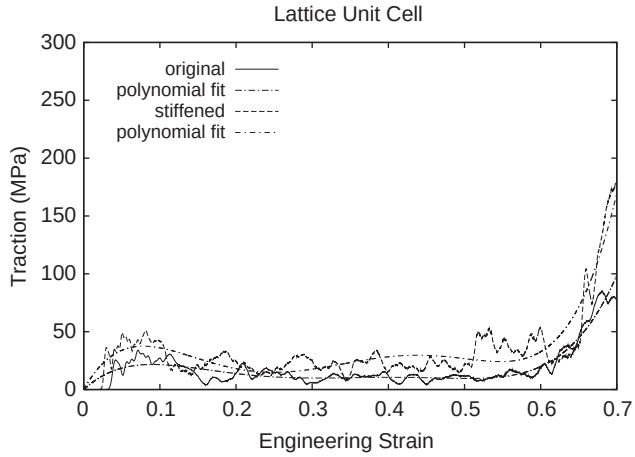

Fig. 11. The effect of doubling the material constants on the response of the lattice microstructure.

remainder of the response appears to generally conform to the doubling rule of thumb.

4. Conclusions and future work

The calculations presented here suggest that particle methods are uniquely suited to performing calculations of the full densification of foam microstructures. The ability to discretize complex geometries and simulate large material deformations

and complex contact has been demonstrated in this work for model microstructures. The simulation results are consistent with various experimental results and engineering guidelines.

Three interesting aspects of foam behavior at the microscale have been examined in this study. The first is that geometric differences in unit cells can lead to unstable snap-through behavior in regular microstructures not present in more disordered unit cells. This result is not unexpected, it is consistent with structural stability theory. However, it serves to demonstrate the range of possible microscale behavior inherent in cellular solids, a term which includes foams, biological materials such as wood, and manufactured materials such as honeycomb. It is clear that materials like honeycombs are geometrically regular while most foamed and biological materials are much less ordered. Collective collapse of rows of cells is well documented in the compression of honeycombs, both statically Gibson and Ashby (1997), Papka and Kyriakides (1998) and dynamically Tanaka et al. (2001), and in the simulation of regular cellular solids Papka and Kyriakides (1998), Meguid et al. (2002). Successive collapse gives rise to, on average, a very flat stress plateau, but with substantial oscillations. Foam bulk behavior is generally much smoother and often monotonic Gibson and Ashby (1997), especially for higher initial relative density materials Smith et al. (2001). Whether this is due to disorder from pore to pore Meguid et al. (2002), Fátima Vaz and Fortes(2001), the absence of severe snap-through behavior at the pore level, or both, appears to be an open question. Available information on the spatial variation of strain in foams suggests smoothly varying heterogeneity for polymeric foams Kinney et al. (2001), Gioia et al. (2001) (somewhat less so for metallic foams Meguid et al. (2002)), rather than dramatic localization. This is an area in which simulations should be able to contribute toward further understanding.

Second, and perhaps most interesting, is the significant level of porosity found even after the foam unit cells have been fully densified. Porosity is not easily removed from these materials under quasi-static deformation. The result is consistent with experimental data Smith et al. (2001). The fact that substantial porosity is retained at full densification indicates that fully densified foams are not well approximated as void free, continuous material. That is, assuming the microstructural network is essentially incompressible is a poor assumption in the densification regime and could result in overlooking important physical processes. For dynamic situations where stress wave propagation is of interest, void space represents an extreme in material property contrast. Reflections at voids result in an irregular wave front and, possibly, dispersion.

Third, an indication of the relationship between foam microstructural properties and bulk properties was found. For the cases simulated, the bulk response generally increased in proportion to the increase in microstructure material properties. Because the result seems plausible it is advanced tentatively as a possible "rule of thumb" which bears further investigation. It should be emphasized that the simulations supporting this relation used, essentially, single pores of foam material. Simulations of much larger unit cells, containing many pores, need to be performed.

To simulate and interpret the microstructural response of *realistic* foams requires (1) representative microstructures for computation, (2) a large scale computation capability in order to handle a microstructure containing 100–1000 pores, (3) a data analysis capability to extract microstructural evolution information. There has been significant progress in all of these areas already. Open cell foam morphology has been extensively studied and techniques have been developed for generating representative structures Kraynik (2003). X-ray tomography has been demonstrated to be capable of generating three-dimensional images of foams Kinney et al. (2001), and provides a data format which should be easily discretized via particle methods. The particle code used for these (serial) calculations is from the University of Utah's Accelerated Strategic Initiative project, and has been ported to both Department of Energy supercomputers and Linux clusters. Image analysis techniques under development have been applied to cellular solids in order to extract geometric features Schlei et al. (2001). Future work will focus on integrating these more advanced capabilities in order to develop a more sophisticated ability to model foams.

The ultimate goal of this research is to facilitate improvement of engineering models of foams. Understanding the relevant mechanics at the microscale, and the influence of various microstructural parameters will enhance our understanding of these important structural materials. However, it is yet another step, generally some sort of homogenization, to extract information which can be used in an engineering model of bulk response. Toward this end, it is useful to have an engineering model in mind. A statistical model has recently been developed which determines foam bulk response based on material parameters and evolution of pore size distribution with deformation Schraad and Harlow (2004). A near term goal of this research is to extract pore size evolution information from computations on realistic foam microstructures, allowing a comparison of the bulk response of the numerical simulation, the engineering model, and experimental data. A first step toward this capability, extraction of porosity evolution, has been demonstrated.

Acknowledgements

The authors would like to acknowledge helpful discussions with M. Schraad and E. Kober, T-Division, LANL, and A. Kraynik and W. Scherzinger, Engineering Sciences, SNL. This work was performed under the auspices of the US Department of Energy at Los Alamos National Laboratory and through the Center for the Simulation of Accidental Fires and Explosions, under Grant W-7405-ENG-48.

References

Atluri, S.N., Zhu, T., 2000. New concepts in meshless methods. Int. J. Numer. Meth. Eng. 47, 537–556.
Babuška, I., Mellenk, J.M., 1997. The partition of unity method. Int. J. Numer. Meth. Eng. 40, 727–758.
Bardenhagen, S.G., Brackbill, J.U., Sulsky, D., 2000. The material-point method for granular materials. Comp. Methods Appl. Mech. Eng. 187, 529–541.

Bardenhagen, S.G., Guilkey, J.E., Roessig, K.M., Brackbill, J.U., Witzel, W.M., Foster, J.C., 2001. An improved contact algorithm for the material point method and application to stress propagation in granular material. Comp. Model. Eng. Sci. 2, 509–522.

Bardenhagen, S.G., Kober, E.M., 2004. The generalized interpolation material point method. Comp. Model. Eng. Sci. 5, 477–496.

Belytschko, T., Krongauz, Y., Organ, D., Fleming, M., Krysl, P., 1996. Meshless methods: an overview and recent developments. Comp. Methods Appl. Mech. Eng. 139, 3–47.

Brackbill, J.U., Kothe, D.B., Ruppel, H.M., 1988. FLIP: A low-dissipation, particle-in-cell method for fluid flow. Comput. Phys. Comm. 48, 25–38.

Burgess, D., Sulsky, D., Brackbill, J.U., 1992. Mass matrix formulation of the FLIP particle-in-cell method. J. Comput. Phys. 103, 1–15.

Chen, C., Lu, T.J., Fleck, N.A., 1999. Effect of imperfections on the yielding of two-dimensional foams. J. Mech. Phys. Solids 47, 2235–2272.

Cummins, S.J., Brackbill, J.U., 2002. An implicit particle-in-cell method for granular materials. J. Comp. Phys. 180, 506–548.

Demkowicz, L., Oden, J.T., 1986. An adaptive characteristic Petrov–Galerkin finite element method for convection-dominated linear and nonlinear parabolic problems in one space variable. J. Comput. Phys. 67, 188–213.

Fátima Vaz, M., Fortes, M.A., 2001. Simulation of cell collapse in the compression of non-uniform cellular solids. Scripta Mater. 45, 375–382.

Gibson, L.J., Ashby, M.F., 1997. Cellular Solids: Structure and Properties. Cambridge University Press, Cambridge.

Gioia, G., Wang, Y., Cuitiño, A.M., 2001. The energetics of heterogeneous deformation in open-cell solid foams. Proc. R. Soc. Lond. A 457, 1079–1096.

Guilkey, J.E., Weiss, J.A., 2003. Implicit time integration for the material point method: quantitative and algorithmic comparisons with the finite element method. Int. J. Numer Meth. Eng. 57, 1323–1338.

Harlow, F.H., 1963. The particle-in-cell computing method for fluid dynamics. Meth. Comput. Phys. 3, 319.

Kinney, J.H., Marshall, G.W., Marshall, S.J., Haupt, D.L., 2001. Three-dimensional imaging of large compressive deformations in elastomeric foams. J. Appl. Polym. Sci. 80, 1746–1755.

Kraynik, A.M., 2003. Foam structure: from soap froth to solid foams. MRS Bull. 28, 275–278.

Legius, H.J.W.M., van den Akker, H.E.A., Narumo, T., 1997. Measurements on wave propagation and bubble and slug velocities in cocurrent upward two-phase flow. Exp. Therm. Fluid Sci. 15, 267–278.

Meguid, S.A., Cheon, S.S., El-Abbasi, N., 2002. Fe modelling of deformation localization in metallic foams. Finite Elements Anal. Design 38, 631–643.

Papka, S.D., Kyriakides, S., 1998. Experiments and full-scale numerical simulations of in-plane crushing of a honeycomb. Acta Mater. 46, 2765–2776.

Schlei, B.R., Prasad, L., Skourikhine, A.N., 2001. Geometric morphology of cellular solids. In: Proceedings of the SPIE—The International Society for Optical Engineering. San Diego, pp. 73–79.

Schraad, M.W., Harlow, F.H., 2004. A stochastic constitutive law for disordered cellular materials. J Mech. Phys. Solids, submitted for publication.

Shulmeister, V., Van der Burg, M.W.D., Van der Giessen, E., Marissen, R., 1998. A numerical study of large deformations of low-density elastomeric open-cell foams. Mech. Mater. 30, 125–140.

Simo, J.C., Hughes, T.J.R., 1998. Computational Inelasticity. Springer, Verlag, New York.

Smith, R.A., Paulus, M.J., Branning, J.M., Phillips, P.J., 2001. X-ray computed tomography on a cellular polysiloxane under compression. J. Cell. Plastics 37, 231–248.

Sulsky, D., Chen, Z., Schreyer, H.L., 1994. A particle method for history-dependent materials. Comp. Methods Appl. Mech. Eng. 118, 179–196.

Sulsky, D., Zhou, S.-J., Schreyer, H.L., 1995. Application of a particle-in-cell method to solid mechanics. Comput. Phys. Commun. 87, 236–252.

Tanaka, K., Nishida, M., Mochida, T., Kousaka, A., 2001. Dynamic response of aluminum honeycombs to in-plane impact loadings. In: Takayama, K., Saito, T., Kleine, H., Timofeev, E. (Eds.), Proceedings of the 24th International Congress on High-Speed Photography and Photonics. pp. 990–997.

Vajjhala, S., Kraynik, A.M., Gibson, L.J., 2000. A cellular solid model for modulus reduction due to resorption of trabeculae in bone. J. Biomech. Eng.-Trans. ASME 122, 511–515.

Wang, Y., Cuitiño, Y., 2000. Three-dimensional nonlinear open-cell foams with large deformations. J. Mech. Phys. Solids 48, 961–988.

Zhong, Z.-H., Mackerie, J., 1994. Contact-impact problems: a review with bibliography. Appl. Mech. Rev. 47, 55–76.

Zhu, H.X., Mills, N.J., Knott, J.F., 1997. Analysis of the high strain compression of open-cell foams. J. Mech. Phys. Solids 45, 1875–1904.

Zhu, H.X., Windle, A.H., 2002. Effects of cell irregularity on the high strain compression of open-cell foams. Acta Mater. 50, 1041–1052.